

hep-ph/0611348
FERMILAB-Pub-06/368-T
CP3-06-16
ILL-(TH)-06-07
September 7, 2018

Production of a W Boson and Two Jets with One b -quark Tag

J. Campbell,¹ R. K. Ellis,² F. Maltoni,³ and S. Willenbrock⁴

¹Department of Physics and Astronomy, University of Glasgow
Glasgow G12 8QQ, United Kingdom

²Theoretical Physics Department, Fermi National Accelerator Laboratory
P. O. Box 500, Batavia, IL 60510

³Institut de Physique Théorique and
Centre for Particle Physics and Phenomenology (CP3)
Université Catholique de Louvain
Chemin du Cyclotron 2
B-1348 Louvain-la-Neuve, Belgium

⁴Department of Physics, University of Illinois at Urbana-Champaign
1110 West Green Street, Urbana, IL 61801

Abstract

The production of a W boson and two jets, at least one of which contains a b quark, is a principal background to single-top production, Higgs production, and signals of new physics at hadron colliders. We present a next-to-leading-order (NLO) calculation of the cross section at the Fermilab Tevatron and the CERN Large Hadron Collider. The NLO cross section differs substantially from that at LO, and we provide a context in which to understand this result.

1 Introduction

Many signals for new physics at hadron colliders involve an electroweak gauge boson (γ, Z, W) and jets, one or more of which contain a heavy quark (c, b). The prime example is the discovery of the top quark via the signal $W + 4j$, where two of the jets contain b quarks [1, 2]. It is important to understand the backgrounds to these signals in as much detail as possible [3]. We have recently completed a next-to-leading-order (NLO) calculation of Z production in association with one or two jets, one (or more) of which contain a heavy quark [4, 5, 6].¹ In this paper we present a NLO calculation of W production in association with two jets, one or more of which contain a b quark. The case of W production in association with one or more jets containing a charm quark is more complicated due to the additional contributions coming from $s \rightarrow Wc$.

The production of a W boson in association with two jets, one or more of which contain a heavy quark, is particularly interesting as it is the principal background to both single-top production [8, 9, 10] and Higgs production (via $q\bar{q}' \rightarrow Wh$) [11, 12], which are currently being sought at the Fermilab Tevatron. Single-top production occurs via both a t -channel process, $qb \rightarrow q't$ [13, 14, 15], and an s -channel process, $q\bar{q}' \rightarrow t\bar{b}$ [16, 17]. In both cases the final state, after top decay, comprises a W boson and two jets, one (t -channel) or both (s -channel) of which contain a b quark. In the case of Higgs production, the final state (after the decay $h \rightarrow b\bar{b}$) comprises a W and two jets, both of which contain a b quark [18, 19]. However, even if both jets contain a b quark, it is more efficient to tag only one of them [12]. Thus in all cases the principal background is W plus two jets, one (or more) of which contain a heavy quark. The signals for single top [20, 21, 22, 23, 24, 25, 26, 27, 28, 29, 30] and Higgs [31, 32, 33] are known at NLO and beyond; our goal is to provide a calculation of the principal background at NLO.

At leading order (LO), there are two processes that produce a W boson and two jets, at least one of which contains a b quark. These are shown in Fig. 1. The process $q\bar{q}' \rightarrow Wb\bar{b}$ yields two b jets, and is already known at NLO [34, 35, 36]. In contrast, the process $bq \rightarrow Wbq'$ yields just one b jet. For a signal with just one b tag, these two processes are comparable at the Tevatron, while at the CERN Large Hadron Collider (LHC) the latter process is dominant [37].

The process $bq \rightarrow Wbq'$ requires further consideration, as it contains a b quark in the initial state. The b distribution in the proton is derived perturbatively via the Dokshitzer-Gribov-Lipatov-Altarelli-Parisi (DGLAP) evolution equations [38, 39]. Alternatively, one may eschew a b distribution function, and use a gluon in the initial state, which then splits to $b\bar{b}$, with one b participating in the hard scattering while the other remains at low transverse momentum; this is shown in Fig. 2 [37]. However, there are two advantages to working with a b distribution function. First, initial-state collinear logarithms, of order $[\alpha_S \ln(M_W/m_b)]^n$, are summed to all orders, yielding a more convergent perturbative expansion. Second, the LO process is simpler, which makes the NLO calculation tractable.

A b distribution function is useful when the scale of the process is much greater than the b mass. In beauty production at HERA, the scale is not much greater than the b mass, and the appropriate description is $\gamma^*g \rightarrow b\bar{b}$ [40]. Thus there is no direct measurement of the b

¹The inclusive production of a Z with one or more heavy quarks is presented in Ref. [7].

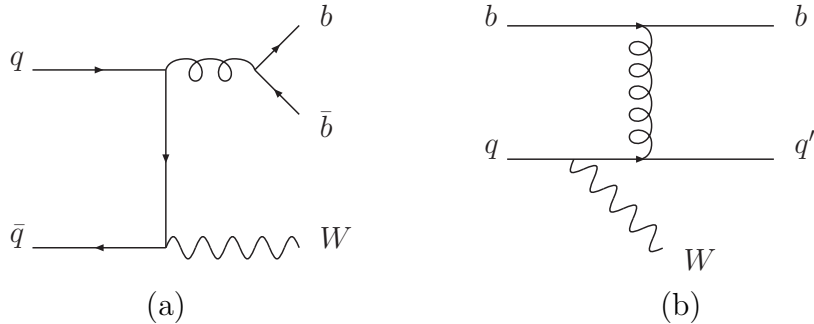


Figure 1: Leading-order processes for the production of a W boson and two jets, at least one of which contains a b quark.

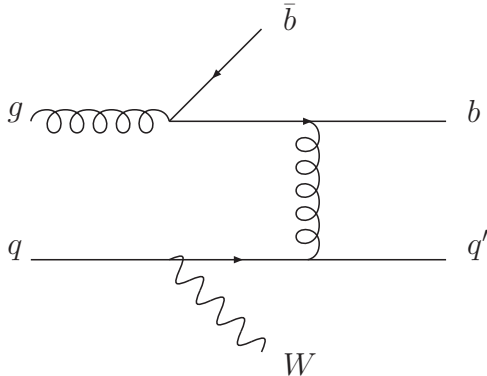


Figure 2: An alternative way of calculating the process in Fig. 1(b).

distribution function at this time. Single-top production (t -channel) may provide the first such measurement.

The paper is organized as follows. In Section 2 we outline the NLO calculation and discuss some of the finer points. The issue of correctly treating the b -quark mass arises in a novel way, and we discuss this in some detail. The results of the calculation are presented in Section 3.

2 Wbj at NLO

The LO cross sections for Wbj and $Wb\bar{b}$, arising from the processes in Figs. 1(b) and 1(a), respectively, are given in parentheses in Table 1. All jets are required to have $p_T > 15$ GeV and $|\eta| < 2$ at the Tevatron, while at the LHC we require $p_T > 25$ GeV and $|\eta| < 2.5$. The jets are required to be separated by $\Delta R_{jj} > 0.7$. As mentioned in the Introduction, these cross sections are comparable at the Tevatron, while Wbj is dominant at the LHC. This qualitative result is already well known from the LO calculation of Ref. [37], which used a gluon in the initial state (Fig. 2) rather than a b quark [Fig. 1(b)]. Our goal is to calculate these cross sections at NLO.

The processes involved in the calculation are as follows:

- $q\bar{q}' \rightarrow Wb\bar{b}$ at tree level [Fig. 1(a)] and one loop
- $bq \rightarrow Wbq'$ at tree level [Fig. 1(b)] and one loop
- $q\bar{q}' \rightarrow Wb\bar{b}g$ at tree level
- $bq \rightarrow Wbq'g$ at tree level
- $gq \rightarrow Wb\bar{b}q'$ at tree level (Fig. 2)
- $bg \rightarrow Wbq\bar{q}'$ at tree level

In all cases $q = u, d, s, c$, and we include Cabibbo-Kobayashi-Maskawa (CKM) mixing. The b -quark mass is neglected throughout (except where noted). The calculation is simpler than the corresponding calculation for ZQj and $ZQ\bar{Q}$ because there are several subprocesses that have no contributing analogue, namely $Qg \rightarrow ZQg$ and $gg \rightarrow ZQ\bar{Q}$ [6]. The analogous processes, $bg \rightarrow Wtg$ and $gg \rightarrow Wt\bar{b}$, yield a top quark in the final state. We do not consider these, or any other processes that yield a top quark, as part of our calculation of the Wbj and $Wb\bar{b}$ backgrounds.

The NLO calculations in this paper were performed with the Monte-Carlo code MCFM [41, 42]. The leading-order calculations were performed both with this code and with MadEvent [43]. The NLO corrections are included in the code MCFM by implementing the virtual helicity amplitudes of Ref. [44]. These are given in the four-dimensional helicity scheme, which is used throughout the calculation. The strong coupling constant is shifted from this scheme to the $\overline{\text{MS}}$ scheme [45]. The real corrections are adapted from Ref. [46] and singularities are handled using the dipole subtraction method [47]. Since the matrix elements contain the decay of the gauge boson into massless particles, the code is general enough to provide results for final states from $W^* \rightarrow \ell\nu$, including the correlation between the W^* spin and the angular distribution of the leptons. For this paper we specialize to the case of an on-shell W boson.

The NLO cross sections are presented in Table 1. To obtain the NLO cross sections for Wbj and $Wb\bar{b}$, which involve the radiation of additional partons, two partons are combined into a single jet by adding their four-momenta if $\Delta R_{jj} < 0.7$. If the combined partons are both b quarks, then the process contributes to the column labeled $W(b\bar{b})j$. This is a $W + 2j$ event in which one jet contains two b quarks, which changes the tagging probability for that jet [48]. It is calculated with a finite b -quark mass ($m_b = 4.75$ GeV) in order to regulate the logarithmic divergence present when the heavy quarks are collinear. If all three partons are well separated, then the process contributes to either $Wb\bar{b}j$ or $Wbjj$.

There is another aspect of the calculation in which the b -quark mass cannot be neglected. If the b quark comes from a final-state virtual gluon splitting to $b\bar{b}$, with the other b quark missed, then the cross section is sensitive to the b -quark mass. This can occur in the NLO processes $q\bar{q}' \rightarrow Wb\bar{b}g$ and $gq \rightarrow Wb\bar{b}q'$, both of which contribute to Wbj when one b quark is missed. We therefore calculated these processes with a finite b -quark mass. In the case of the process $gq \rightarrow Wb\bar{b}q'$, which involves the splitting $g \rightarrow b\bar{b}$ in the initial state (see Fig. 2) as well as the final state, this requires that we abandon the dipole subtraction method in

favor of subtracting the mass singularity via the truncated b distribution function [38, 39]

$$\tilde{b}(x, \mu) = \frac{\alpha_S(\mu)}{2\pi} \ln\left(\frac{\mu^2}{m_b^2}\right) \int_x^1 \frac{dy}{y} P_{qg}\left(\frac{x}{y}\right) g(y, \mu) \quad (1)$$

where $P_{qg}(z) = \frac{1}{2}[z^2 + (1-z)^2]$ is the DGLAP splitting function. The counterterm is constructed by calculating $\tilde{b}q \rightarrow Wbq'$; this cancels the initial-state logarithmic dependence on the b -quark mass in $gq \rightarrow Wb\bar{b}q'$, and yields a cross section in the $\overline{\text{MS}}$ factorization scheme.

It is interesting to compare the LO result for Wbj with a calculation based on $gq \rightarrow Wq'\bar{b}\bar{b}$ (Fig. 2) [37], which does not use a b distribution function. With the same parameters as Table 1, and using $m_b = 4.75$ GeV and CTEQ6L1 parton distribution functions [49], we find a cross section of 1.92 pb at the Tevatron. This is to be compared with 1.06 pb using $bq \rightarrow Wbq'$, and serves as a rough check of the formalism. Both of these numbers are LO and very scale dependent, so one should expect only qualitative agreement.² The result at the LHC ($W^+ + W^-$) is 81 pb, which is to be compared with the 87.3 pb result obtained using $bq \rightarrow Wbq'$ (see Table 1). In any case, the NLO results presented in this paper should be more accurate than any of these LO results.

We checked that the effect of the heavy-quark mass is small if all b quarks are at high p_T by comparing $Wb\bar{b}$ at tree level with and without a finite quark mass. With the cuts used in this paper, we find a reduction of the $Wb\bar{b}$ cross section by about 7% at the Tevatron ($p_T > 15$ GeV) and 2% at the LHC ($p_T > 25$ GeV). This is the same as the result found for the effect of the b -quark mass on the full NLO calculation at the Tevatron [36], which suggests that the effect of the b -quark mass can be divined from a LO calculation. We found that the heavy-quark mass is a similarly small effect for $Wb\bar{b}j$ at tree level, as expected.

We also list in Table 1 the LO (in parentheses) and NLO cross sections for Wjj [35, 50], and the LO cross section for $Wjjj$. We ignore CKM mixing, which is a negligible effect at LO, and is therefore also negligible at NLO. In these cross sections we have included the contribution from light partons as well as heavy quarks (c, b). Thus, for example, the fraction of $W + 2j$ events in which only one of the jets can be tagged as b jet is given by $[Wbj + W(b\bar{b})j]/Wjj$.

3 Results

The results in Table 1 are remarkable. First we see that, at NLO, the cross sections for Wbj and $Wb\bar{b}$ are comparable at the Tevatron. Thus both final states are important backgrounds to single top and Higgs. At the LHC, Wbj is much larger than $Wb\bar{b}$. At both machines, the correction to Wbj is large (for $\mu_F = \mu_R = M_W$), about a factor of 1.9 at the LHC and a factor of 2.4 at the Tevatron. The correction is larger at the Tevatron because $Wb\bar{b}$, which is comparable in size, feeds into the Wbj column at NLO when one of the b quarks is outside the fiducial region ($p_T > 15$ GeV, $|\eta| < 2$).

²Including the uncertainties due to the independent variation of the renormalization and factorization scales from $M_W/2$ to $2M_W$, the cross sections are $1.92^{+0.84}_{-0.51} +0.22_{-0.15}$ pb for $gq \rightarrow Wq'\bar{b}\bar{b}$ and $1.06^{+0.28}_{-0.20} +0.03_{-0.07}$ pb for $bq \rightarrow Wbq'$

The correction to $Wb\bar{b}$ is significant at both machines, but more modest than that of Wbj , again for $\mu_F = \mu_R = M_W$. At the LHC the cross section for $Wb\bar{b}j$ is comparable to that of $Wb\bar{b}$, which calls into question the reliability of perturbation theory. However, $Wb\bar{b}j$ is also a correction to Wbj , and when compared with that LO cross section it is a modest correction. Nevertheless, it does mean that when demanding two b quarks in the final state, the processes $Wb\bar{b}$ and $Wb\bar{b}j$ are comparable at the LHC. The latter is only known at LO and therefore has a large uncertainty. This is reflected by the large scale dependence associated with this process, as discussed in Refs. [35, 36].

Using the results in Table 1, we construct a set of inclusive cross sections, presented in Table 2. Displayed this way, the radiative corrections to the cross sections are even more significant, especially for $Wb\bar{b} + X$ at the LHC, where the NLO cross section is about 2.7 times the LO cross section. However, the proper way to regard this is that a new process enters at NLO, namely $gq \rightarrow Wb\bar{b}q'$ (see Fig. 2), which is also a correction to the much larger LO process $bq \rightarrow Wbq'$, as discussed in the previous paragraph. We also list the uncertainties from varying the renormalization scale from $M_W/2$ to $2M_W$ while keeping the factorization scale fixed at M_W , from varying the factorization scale from $M_W/2$ to $2M_W$ while keeping the renormalization scale fixed at M_W , and from varying the parton distribution functions [49]. The largest uncertainty is from varying the renormalization scale, since the process under consideration is of order α_S^2 at leading order.

We show in Figs. 3 and 4 the renormalization- and factorization-scale dependence at LO and NLO for the inclusive $Wbj + X$ cross section at the Tevatron and the LHC, respectively. At the Tevatron, there is almost no reduction of the renormalization-scale dependence at NLO. This supports our earlier argument that part of the source of the large NLO correction to this process is that the process $Wb\bar{b}j$ contributes when one of the b jets is missed. Since this is a tree-level process, it has a large renormalization-scale dependence. There is only a mild reduction of the renormalization-scale dependence at the LHC. At both machines there is a mild reduction of the factorization-scale dependence.

Using the code MCFM [41, 42], we are able to plot any desired distribution at both LO and NLO. For example, we show in Fig. 5 the exclusive NLO differential cross section at the Tevatron for $Wb\bar{b}$, Wbj , and $W(b\bar{b})j$, versus the transverse momentum (p_T) of the jet with the highest p_T . For Wbj , the highest- p_T jet contains a b quark 48% of the time; for $W(b\bar{b})j$, the percentage is 63%. The $W(b\bar{b})j$ cross section, which first arises at NLO, has a very different shape from the other two, and is only significant at high p_T .

The lower histogram in Fig. 5 shows the ratio of the NLO and LO cross sections. We see that there is a change in shape of the Wbj and $Wb\bar{b}$ differential cross sections at NLO, with relatively more events at low p_T . There is also an enhancement of the Wbj cross section at high p_T , due to the process $q\bar{q} \rightarrow Wb\bar{b}j$ with one b missed.

We show in Fig. 6 the exclusive NLO transverse momentum distribution of the charged lepton from W decay at the Tevatron. We again see a change in shape at NLO, with relatively more events at low p_T for $Wb\bar{b}$, and relatively more events at high p_T for Wbj , the latter again due to the process $q\bar{q} \rightarrow Wb\bar{b}j$ with one b missed. This plot demonstrates the ability of MCFM to calculate quantities involving the decay products of the W boson while correctly treating the correlation between the angular distribution of the decay products and the W spin. The W boson is treated as on-shell in these plots, but MCFM is flexible enough to allow for off-shell W bosons as well.

Table 1: Exclusive cross sections (pb) for W boson plus two (or more) jets, with at least one b jet, at the Tevatron ($\sqrt{s} = 1.96$ TeV $p\bar{p}$, $p_T > 15$ GeV and $|\eta| < 2$) and LHC ($\sqrt{s} = 14$ TeV pp , $p_T > 25$ GeV and $|\eta| < 2.5$). Two final-state partons are merged into a single jet if $\Delta R_{jj} < 0.7$. No branching ratios or tagging efficiencies are included. The labels on the columns have the following meaning: Wbj = exactly two jets, one of which contains a b quark; $Wb\bar{b}$ = exactly two jets, both of which contain a b quark; $W(b\bar{b})j$ = exactly two jets, one of which contains two b quarks; $Wbjj$ = exactly three jets, one of which contains a b quark; $Wb\bar{b}j$ = exactly three jets, two of which contain a b quark. For the last set of processes, which include both light and heavy partons in the final state, the labels mean: Wjj = exactly two jets; $Wjjj$ = exactly three jets. For Wbj , $Wb\bar{b}$, and Wjj , both the leading-order (in parentheses) and next-to-leading-order cross sections are given. The CTEQ6M parton distribution functions are used throughout, except for the LO cross sections in parentheses, where CTEQ6L1 is used [49]. The factorization and renormalization scales are chosen as $\mu_F = \mu_R = M_W$.

Collider	Cross sections (pb)				
	Wbj	$Wb\bar{b}$	$W(b\bar{b})j$	$Wbjj$	$Wb\bar{b}j$
TeV $W^+(=W^-)$	(1.06) 2.54	(2.48) 3.14	0.89	0.18	0.65
LHC W^+	(51.7) 96.2	(9.5) 14.3	27.0	13.8	11.6
LHC W^-	(35.6) 66.4	(6.6) 9.6	19.0	9.3	7.6
	Wjj			$Wjjj$	
TeV $W^+(=W^-)$	(261) 290			39	
LHC W^+	(4990) 4170			1280	
LHC W^-	(3650) 3030			890	

We show in Fig. 7 the exclusive NLO di-jet invariant mass at the Tevatron. Both $Wb\bar{b}$ and Wbj are enhanced at low invariant masses at NLO. The process $W(b\bar{b})j$ is significant at high invariant mass. All three processes are numerically important as backgrounds to the search for a Higgs boson via the process $q\bar{q} \rightarrow Wh \rightarrow Wb\bar{b}$. For example, the integrated cross sections in the region $110 \text{ GeV} < m_{jj} < 130 \text{ GeV}$ are 130 fb for Wbj , 95 fb for $Wb\bar{b}$, and 75 fb for $W(b\bar{b})j$.

We show in Figs. 8,9, 10 the same distributions at the LHC, but this time for the inclusive cross sections, rather than exclusive. At the LHC, the process $Wbj + X$ is dominant, while $Wb\bar{b} + X$ and $W(b\bar{b})j$ are comparable. There is little change in shape of the distributions at NLO, with the exception of the p_T spectrum of the highest p_T jet, which is enhanced at high p_T for $Wb\bar{b} + X$. The di-jet invariant mass distribution also shows an enhancement at low values of the invariant mass, but not at values relevant for the Higgs search.

The code MCFM is publicly available [42], and one can generate any desired distribution.

Table 2: Inclusive cross sections (pb) for W boson plus two (or more) jets, with at least one b jet, at the Tevatron ($\sqrt{s} = 1.96$ TeV $p\bar{p}$, $p_T > 15$ GeV and $|\eta| < 2$) and LHC ($\sqrt{s} = 14$ TeV pp , $p_T > 25$ GeV and $|\eta| < 2.5$). Two final-state partons are merged into a single jet if $\Delta R_{jj} < 0.7$. No branching ratios or tagging efficiencies are included. The labels on the columns have the following meaning: $Wbj + X$ = at least two jets, one of which contains a b quark; $Wb\bar{b} + X$ = at least two jets, two of which contain a b quark; $W(b\bar{b})j$ = two jets, one of which contains two b quarks. The label $Wjj + X$ = at least two jets, containing both light and heavy partons. For $Wbj + X$, $Wb\bar{b} + X$, and $Wjj + X$, both the leading-order (in parentheses) and next-to-leading-order cross sections are given. The CTEQ6M parton distribution functions are used throughout, except for the LO cross sections in parentheses, where CTEQ6L1 is used [49]. The factorization and renormalization scales are chosen as $\mu_F = \mu_R = M_W$. The uncertainties are from the variation of the renormalization scale, the factorization scale, and the parton distribution functions, respectively.

Collider	Cross sections (pb)		
	$Wbj + X$	$Wb\bar{b} + X$	$W(b\bar{b})j$
TeV $W^+(=W^-)$	(1.06) $2.72^{+0.68}_{-0.50} {}^{+0.01}_{-0.04} {}^{+0.09}_{-0.09}$	(2.49) $3.79^{+0.56}_{-0.47} {}^{+0.12}_{-0.08} {}^{+0.11}_{-0.11}$	$0.89^{+0.36}_{-0.23} {}^{+0.10}_{-0.07} {}^{+0.03}_{-0.03}$
LHC W^+	(51.7) $110^{+23}_{-18} {}^{+11}_{-17} {}^{+3.6}_{-3.6}$	(9.5) $25.9^{+6.2}_{-5.1} {}^{+0}_{-0.3} {}^{+0.6}_{-0.6}$	$27.0^{+11}_{-7.1} {}^{+0.1}_{-0.3} {}^{+0.9}_{-0.9}$
LHC W^-	(35.6) $75.7^{+17}_{-12} {}^{+7.3}_{-9.5} {}^{+2.6}_{-2.6}$	(6.6) $17.2^{+4.2}_{-3.3} {}^{+0.2}_{-0.5} {}^{+0.5}_{-0.5}$	$19.0^{+7.7}_{-5.0} {}^{+0.1}_{-0.3} {}^{+0.7}_{-0.7}$
	$Wjj + X$		
TeV $W^+(=W^-)$	(261) $329^{+30}_{-32} {}^{+6}_{-6} {}^{+7}_{-7}$		
LHC W^+	(4990) $5450^{+410}_{-480} {}^{+70}_{-0} {}^{+190}_{-190}$		
LHC W^-	(3650) $3920^{+300}_{-310} {}^{+60}_{-10} {}^{+150}_{-150}$		

We hope the calculation outlined in this paper is useful to better understand the backgrounds to single-top production, Higgs production, and signals of new physics at the Tevatron and the LHC.

Acknowledgments

We are grateful for conversations and correspondence with C. Ciobanu, J. Ellison, A. Heinson, T. Junk, T. Liss, T. McElmurry, F. Olness, K. Pitts, and R. Schwienhorst. J. C. and S. W. thank the Aspen Center for Physics for hospitality. This work was supported in part by the U. S. Department of Energy under contracts Nos. DE-AC02-76CH03000 and DE-FG02-91ER40677.

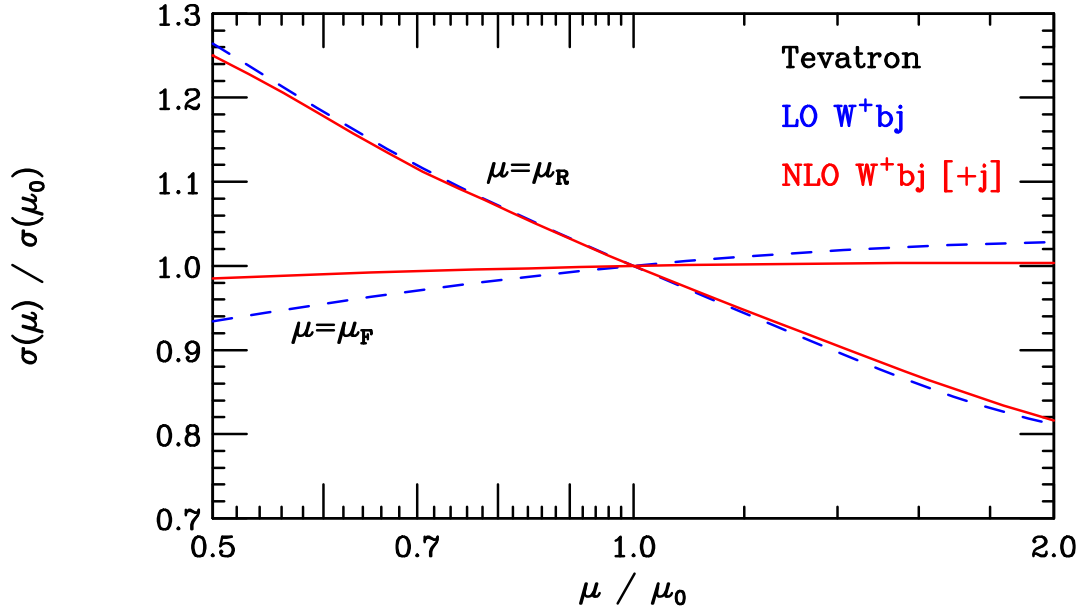


Figure 3: Renormalization- and factorization-scale dependence of the inclusive $Wbj+X$ cross section at LO (dashed) and NLO (solid) at the Tevatron. The cross section is normalized to its value at the reference scale $\mu_0 = M_W$.

References

- [1] F. Abe *et al.* [CDF Collaboration], Phys. Rev. Lett. **74**, 2626 (1995) [arXiv:hep-ex/9503002].
- [2] S. Abachi *et al.* [D0 Collaboration], Phys. Rev. Lett. **74**, 2632 (1995) [arXiv:hep-ex/9503003].
- [3] D. Acosta *et al.* [CDF Collaboration], Phys. Rev. D **65**, 052007 (2002) [arXiv:hep-ex/0109012].
- [4] J. M. Campbell and R. K. Ellis, Phys. Rev. D **62**, 114012 (2000) [arXiv:hep-ph/0006304].
- [5] J. Campbell, R. K. Ellis, F. Maltoni and S. Willenbrock, Phys. Rev. D **69**, 074021 (2004) [arXiv:hep-ph/0312024].
- [6] J. Campbell, R. K. Ellis, F. Maltoni and S. Willenbrock, Phys. Rev. D **73**, 054007 (2006) [arXiv:hep-ph/0510362].
- [7] F. Maltoni, T. McElmurry and S. Willenbrock, Phys. Rev. D **72**, 074024 (2005) [arXiv:hep-ph/0505014].
- [8] D. Acosta *et al.* [CDF Collaboration], Phys. Rev. D **71**, 012005 (2005) [arXiv:hep-ex/0410058].
- [9] V. M. Abazov *et al.* [D0 Collaboration], Phys. Lett. B **622**, 265 (2005) [arXiv:hep-ex/0505063].

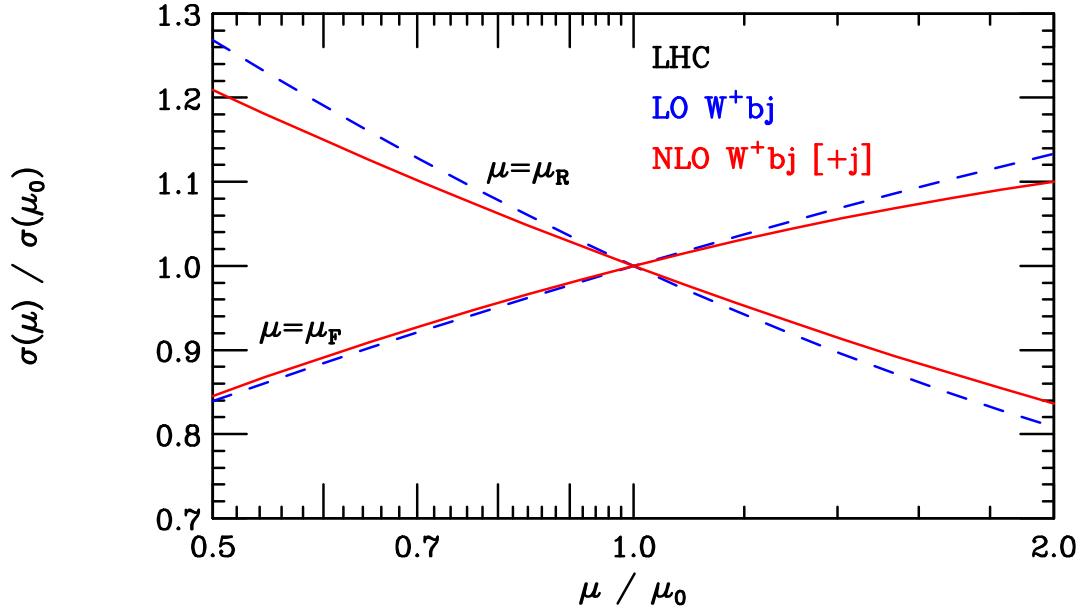


Figure 4: Same as Fig. 3, but at the LHC.

- [10] V. M. Abazov *et al.* [D0 Collaboration], arXiv:hep-ex/0604020.
- [11] V. M. Abazov *et al.* [D0 Collaboration], Phys. Rev. Lett. **94**, 091802 (2005) [arXiv:hep-ex/0410062].
- [12] D. Acosta *et al.* [CDF Collaboration], Phys. Rev. Lett. **95**, 051801 (2005) [arXiv:hep-ex/0503039].
- [13] S. S. D. Willenbrock and D. A. Dicus, Phys. Rev. D **34**, 155 (1986).
- [14] C. P. Yuan, Phys. Rev. D **41**, 42 (1990).
- [15] R. K. Ellis and S. J. Parke, Phys. Rev. D **46**, 3785 (1992).
- [16] S. Cortese and R. Petronzio, Phys. Lett. B **253**, 494 (1991).
- [17] T. Stelzer and S. Willenbrock, Phys. Lett. B **357**, 125 (1995) [arXiv:hep-ph/9505433].
- [18] A. Stange, W. J. Marciano and S. Willenbrock, Phys. Rev. D **49**, 1354 (1994) [arXiv:hep-ph/9309294].
- [19] A. Stange, W. J. Marciano and S. Willenbrock, Phys. Rev. D **50**, 4491 (1994) [arXiv:hep-ph/9404247].
- [20] G. Bordes and B. van Eijk, Nucl. Phys. B **435**, 23 (1995).
- [21] M. C. Smith and S. Willenbrock, Phys. Rev. D **54**, 6696 (1996) [arXiv:hep-ph/9604223].
- [22] T. Stelzer, Z. Sullivan and S. Willenbrock, Phys. Rev. D **56**, 5919 (1997) [arXiv:hep-ph/9705398].

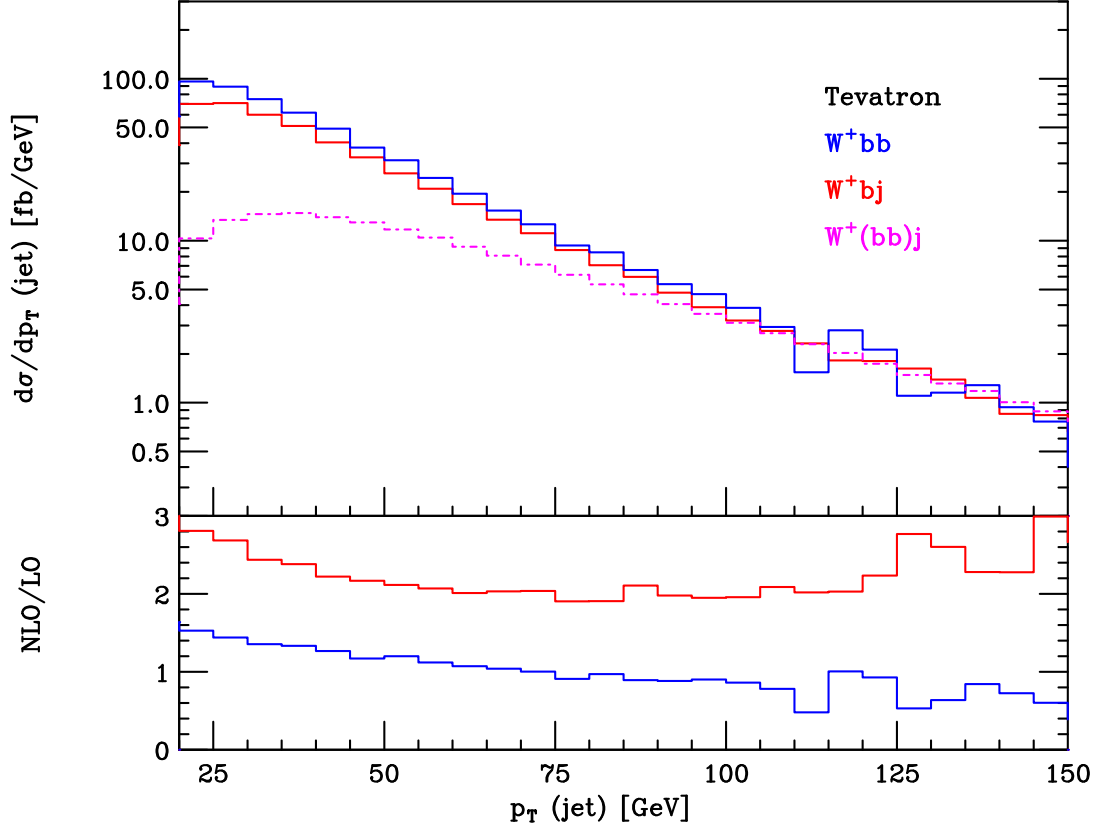


Figure 5: Exclusive NLO differential cross sections at the Tevatron ($\sqrt{s} = 1.96$ TeV $p\bar{p}$, $p_T > 15$ GeV, $|\eta| < 2$, $\Delta R_{jj} > 0.7$) for Wbb (blue or black) and Wbj (red or gray), versus the transverse momentum (p_T) of the highest- p_T jet. Also shown is the distribution for the NLO process $W(bb)j$ (magenta or light gray, dot-dashed), in which a jet contains two b quarks. The lower histogram shows the ratio of the NLO and LO cross sections.

- [23] K. G. Chetyrkin and M. Steinhauser, Phys. Lett. B **502**, 104 (2001) [arXiv:hep-ph/0012002].
- [24] B. W. Harris, E. Laenen, L. Phaf, Z. Sullivan and S. Weinzierl, Phys. Rev. D **66**, 054024 (2002) [arXiv:hep-ph/0207055].
- [25] Q. H. Cao and C. P. Yuan, Phys. Rev. D **71**, 054022 (2005) [arXiv:hep-ph/0408180].
- [26] Q. H. Cao, R. Schwienhorst and C. P. Yuan, Phys. Rev. D **71**, 054023 (2005) [arXiv:hep-ph/0409040].
- [27] Z. Sullivan, Phys. Rev. D **70**, 114012 (2004) [arXiv:hep-ph/0408049].
- [28] J. Campbell, R. K. Ellis and F. Tramontano, Phys. Rev. D **70**, 094012 (2004) [arXiv:hep-ph/0408158].
- [29] Q. H. Cao, R. Schwienhorst, J. A. Benitez, R. Brock and C. P. Yuan, Phys. Rev. D **72**, 094027 (2005) [arXiv:hep-ph/0504230].

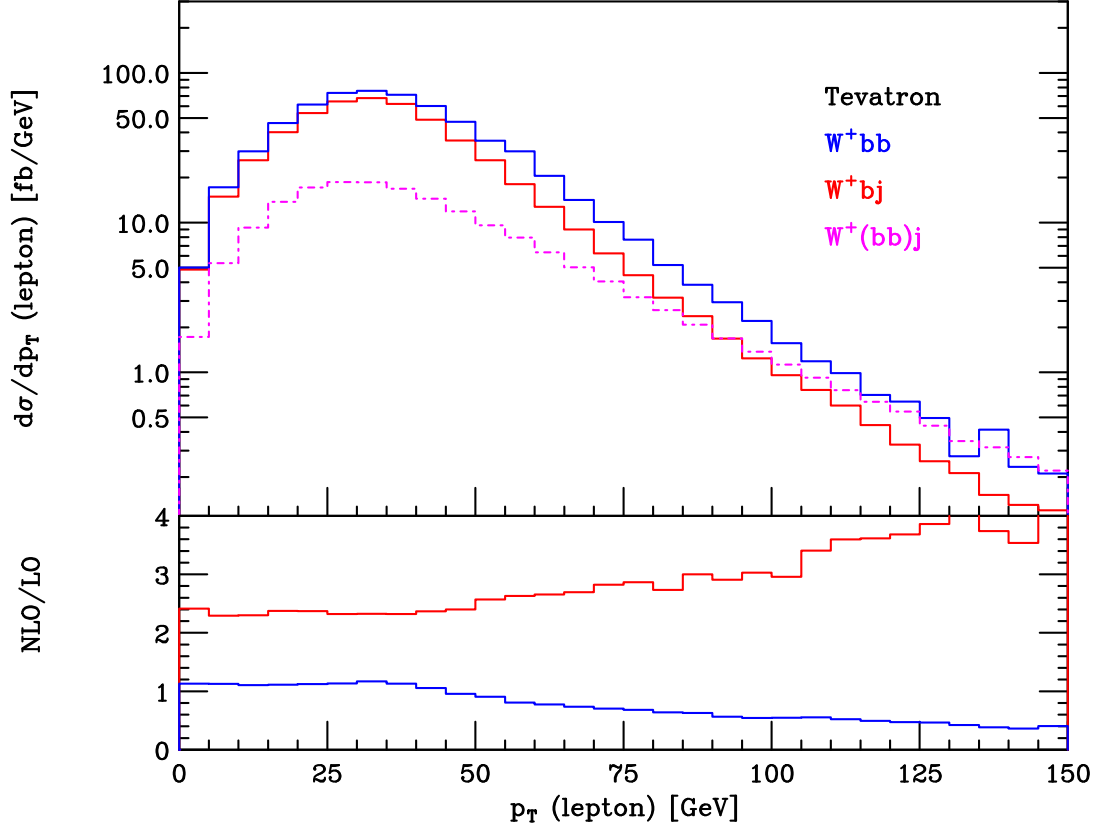


Figure 6: Same as Fig. 5, but for the charged lepton from W decay.

- [30] S. Frixione, E. Laenen, P. Motylinski and B. R. Webber, JHEP **0603**, 092 (2006) [arXiv:hep-ph/0512250].
- [31] T. Han and S. Willenbrock, Phys. Lett. B **273**, 167 (1991).
- [32] O. Brein, A. Djouadi and R. Harlander, Phys. Lett. B **579**, 149 (2004) [arXiv:hep-ph/0307206].
- [33] M. L. Ciccolini, S. Dittmaier and M. Kramer, Phys. Rev. D **68**, 073003 (2003) [arXiv:hep-ph/0306234].
- [34] R. K. Ellis and S. Veseli, Phys. Rev. D **60**, 011501 (1999) [arXiv:hep-ph/9810489].
- [35] J. Campbell, R. K. Ellis and D. L. Rainwater, Phys. Rev. D **68**, 094021 (2003) [arXiv:hep-ph/0308195].
- [36] F. Febres Cordero, L. Reina and D. Wackerth, Phys. Rev. D **74**, 034007 (2006) [arXiv:hep-ph/0606102].
- [37] M. L. Mangano, M. Moretti and R. Pittau, Nucl. Phys. B **632**, 343 (2002) [arXiv:hep-ph/0108069].

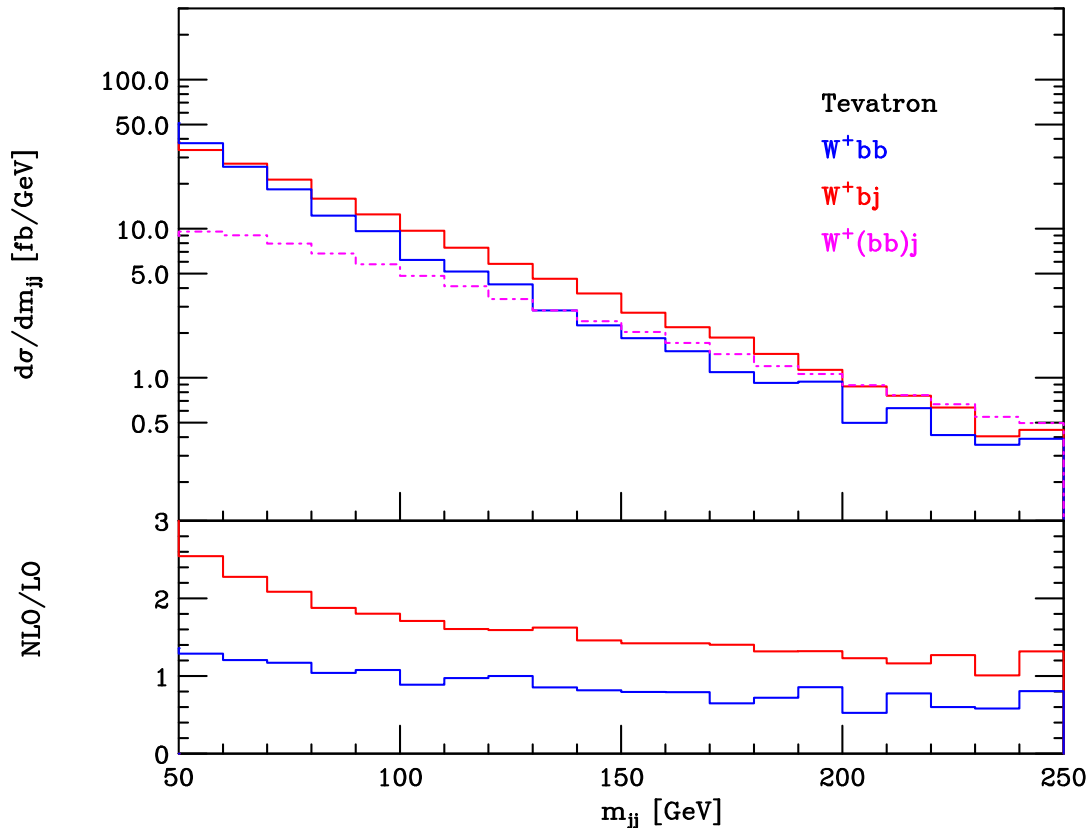


Figure 7: Same as Fig. 5, but for the di-jet invariant mass.

- [38] M. A. G. Aivazis, J. C. Collins, F. I. Olness and W. K. Tung, Phys. Rev. D **50**, 3102 (1994) [arXiv:hep-ph/9312319].
- [39] J. C. Collins, Phys. Rev. D **58**, 094002 (1998) [arXiv:hep-ph/9806259].
- [40] C. Grab [H1 and ZEUS Collaborations], Acta Phys. Polon. B **37**, 773 (2006).
- [41] R. K. Ellis *et al.* [QCD Tools Working Group], arXiv:hep-ph/0011122.
- [42] J. Campbell and R. K. Ellis, MCFM - Monte Carlo for FeMtobarn processes, <http://mcfm.fnal.gov/>.
- [43] F. Maltoni and T. Stelzer, JHEP **0302**, 027 (2003) [arXiv:hep-ph/0208156].
- [44] Z. Bern, L. J. Dixon and D. A. Kosower, Nucl. Phys. B **513**, 3 (1998) [arXiv:hep-ph/9708239].
- [45] S. Catani, M. H. Seymour and Z. Trocsanyi, Phys. Rev. D **55**, 6819 (1997) [arXiv:hep-ph/9610553].
- [46] Z. Nagy and Z. Trocsanyi, Phys. Rev. D **59**, 014020 (1999) [Erratum-ibid. D **62**, 099902 (2000)] [arXiv:hep-ph/9806317].

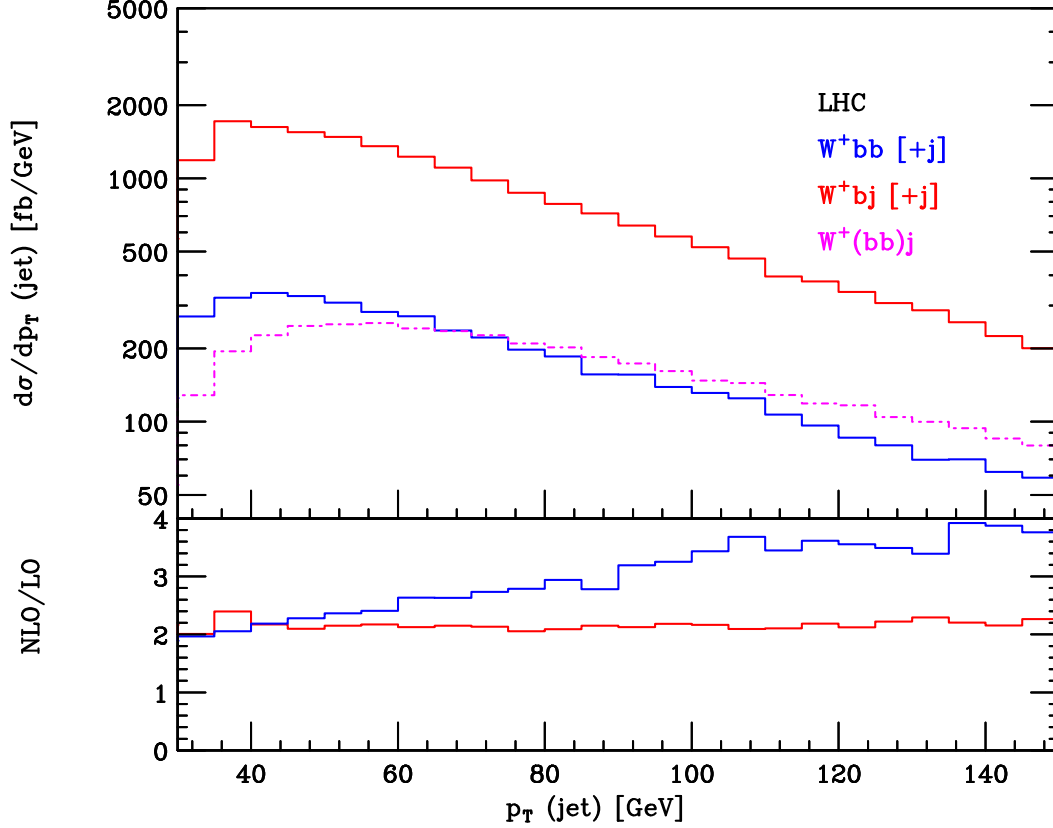


Figure 8: Inclusive NLO differential cross sections at the LHC ($\sqrt{s} = 14$ TeV pp , $p_T > 25$ GeV, $|\eta| < 2.5$, $\Delta R_{jj} > 0.7$) for $Wbb[+j]$ (blue or black) and $Wbj[+j]$ (red or gray), versus the transverse momentum (p_T) of the highest- p_T jet. Also shown is the distribution for the NLO process $W(b\bar{b})j$ (magenta or light gray, dot-dashed), in which a jet contains two b quarks. The lower histogram shows the ratio of the NLO and LO cross sections.

- [47] S. Catani and M. H. Seymour, Nucl. Phys. B **485**, 291 (1997) [Erratum-ibid. B **510**, 503 (1997)] [arXiv:hep-ph/9605323].
- [48] D. Acosta *et al.* [CDF Collaboration], Phys. Rev. D **71**, 092001 (2005) [arXiv:hep-ex/0412006].
- [49] J. Pumplin, D. R. Stump, J. Huston, H. L. Lai, P. Nadolsky and W. K. Tung, JHEP **0207**, 012 (2002) [arXiv:hep-ph/0201195].
- [50] J. Campbell and R. K. Ellis, Phys. Rev. D **65**, 113007 (2002) [arXiv:hep-ph/0202176].

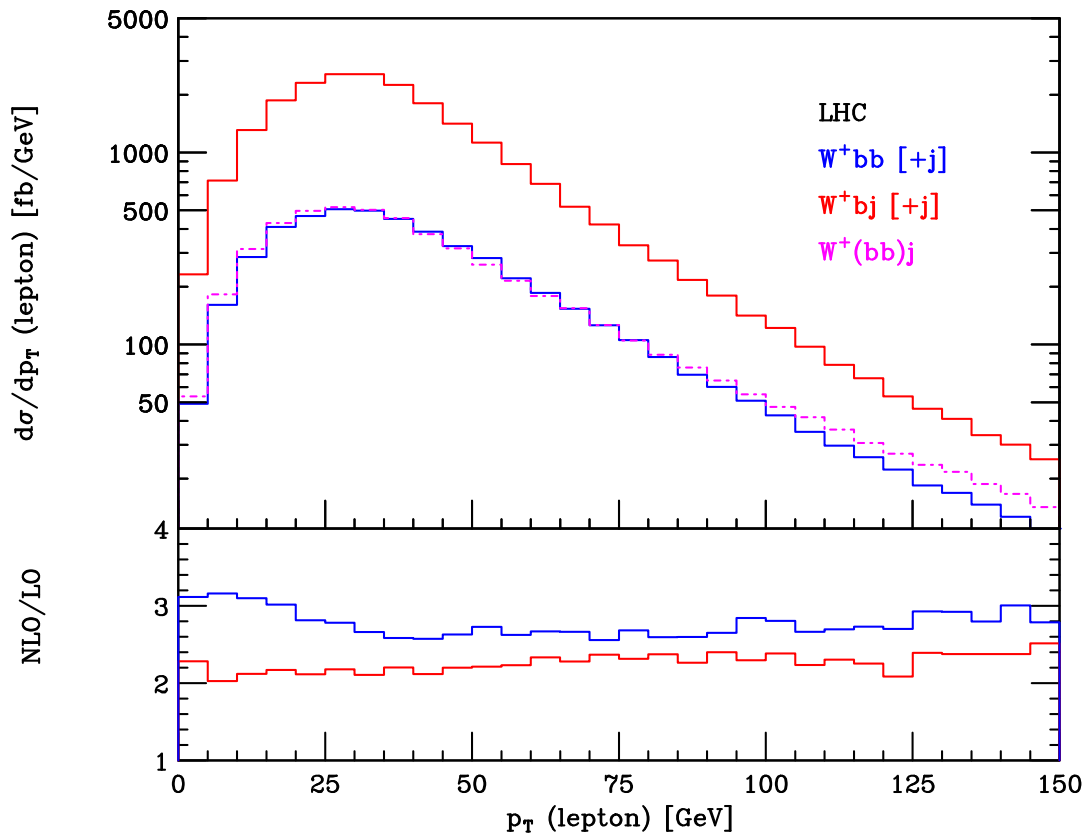


Figure 9: Same as Fig. 8, but for the charged lepton from W decay.

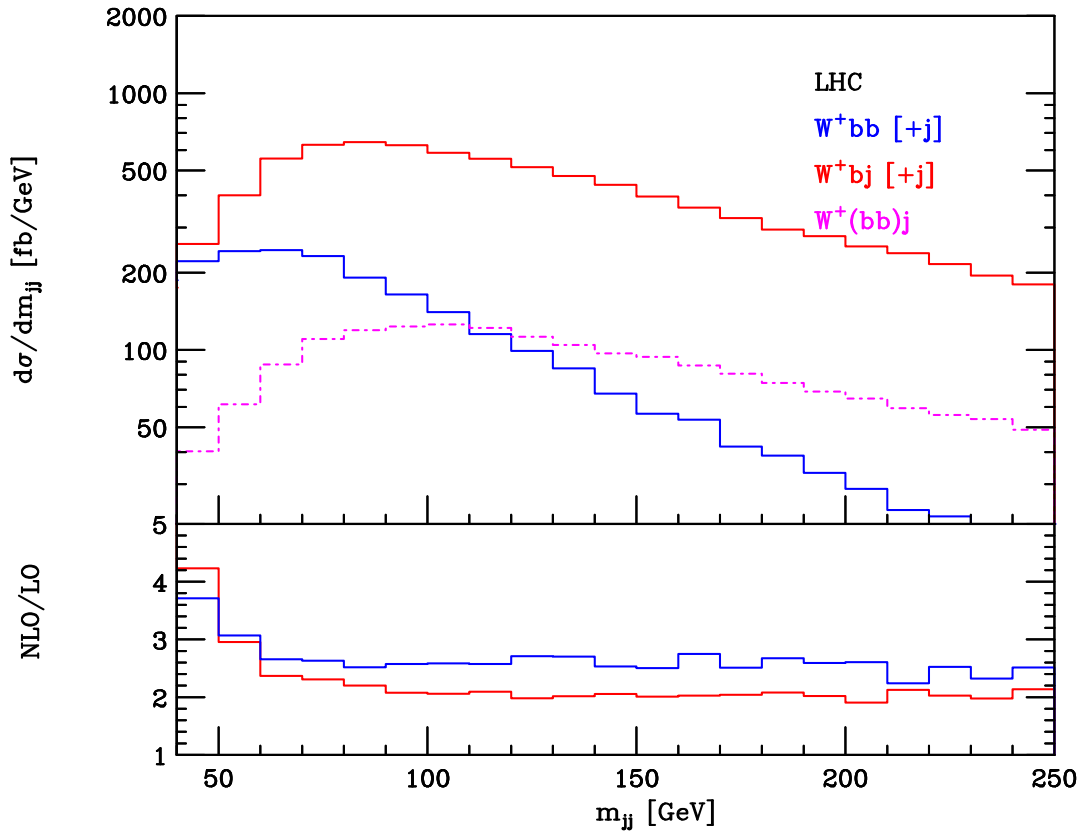


Figure 10: Same as Fig. 8, but for the di-jet invariant mass. For $Wbb[+j]$, the invariant mass is that of the two b jets; for $Wbj[+j]$, the invariant mass is that of the b jet and the other jet with the higher p_T .